Available online at www.sciencedirect.com

ScienceDirect

Ceramics International 40 (2014) 4707–4715

CERAMICS INTERNATIONAL

www.elsevier.com/locate/ceramint

Effects of the single layer CVD SiC interphases on mechanical properties of mullite fiber-reinforced mullite matrix composites fabricated via a sol–gel process

Yi Wang*, Haifeng Cheng, Jun Wang

Science and Technology on Advanced Ceramic Fibers and Composites Laboratory, National University of Defense Technology, Changsha 410073, Hunan, PR China

Received 11 August 2013; received in revised form 31 August 2013; accepted 3 September 2013
Available online 9 September 2013

Abstract

Due to the degradation of mechanical properties of mullite fiber-reinforced mullite matrix (Mu_f/Mu) composites with pyrocarbon (PyC) and BN interphases under an oxidation environment, single layer SiC interphases prepared by a chemical vapor deposition (CVD) process were employed. Effects of the CVD SiC interphases on mechanical properties and interfacial characteristics of Mu_f/Mu composites fabricated via a sol–gel process were investigated. The results show that the composites with CVD SiC interphases exhibit an obvious toughened fracture behavior, and the flexural strength is about 2.67 times that of the composites without SiC interphases. Microstructure analysis reveals that SiC interphases play a key part in protecting fibers from being damaged during the fabrication process of the composites, and weakening bonding between fibers and matrix, which are both beneficial to the improvement in mechanical properties of the composites. Flexural strength of the composites with SiC interphases after oxidation decreases by about 25.4%.

Keywords: A. Sol–gel process; B. Composites; C. Mechanical properties; D. Mullite; SiC interphases

1. Introduction

For high temperature applications, mullite ($3Al_2O_3 \cdot 2SiO_2$) ceramic has received considerable attention in the past decades due to its outstanding properties, such as good chemical and thermal stability, low thermal expansion coefficient and conductivity, low dielectric constant and high creep resistance [1,2]. However, the application of mullite ceramic is largely limited by its low strength and fracture toughness [3]. Continuous fiber is one of the most effective reinforcements for mullite ceramic. Several continuous fibers have been introduced into the mullite matrix, e.g. C_f/Mu, SiC_f/Mu, Al_2O_{3f}/Mu, Mu_f/Mu, etc. [4–7]. Hereinto, Mu_f/Mu composites usually have low strength due to the strong bonding between fibers and matrix, and decreasing of the fiber strength during the fabrication process [8,9]. Therefore, several interphase materials, such as BN, PyC, BN/SiC, monazite [10–12], have been used to weaken interfacial bonding. But the single layer SiC interphases have never been used in Mu_f/Mu composites.

The purpose of this paper is to investigate the effects of the single layer CVD SiC interphases on mechanical properties and interfacial characteristics of Mu_f/Mu composites fabricated via a sol–gel process.

2. Experimental procedure

2.1. Raw materials

The reinforcements used to prepare Mu_f/Mu composites were twill-woven mullite fiber fabrics (ALF 3025T-FB3, from Nitivy ALF Company, Japan). The mullite fiber preform was 3D-sewed by 8 layer mullite fiber fabrics using mullite fiber yarns and the fiber volume fraction was about 41.5%. Diphasic mullite sol, the precursor of the mullite matrix, was prepared by blending a silica sol and an alumina sol (both from

*Corresponding author. Tel./fax: +86 731 84576440.
E-mail address: wycfcnudt@163.com (Y. Wang).

0272-8842/$ - see front matter © 2013 Elsevier Ltd and Techna Group S.r.l. All rights reserved.
http://dx.doi.org/10.1016/j.ceramint.2013.09.012

Snowchemical S&T Co., Ltd., China) in proportion to their contents in the chemical composition of $3Al_2O_3 \cdot 2SiO_2$ (3/2-mullite) through mechanical stirring lasting for 0.5–1 h. The density and viscosity of the mullite sol are 1.15 g/cm^3 and 6 mPa s, respectively. The ceramic yield is about 24.1 wt% at 1300 °C and pH is 5.0.

2.2. Materials preparation

Methyltrichlorosilane (MTS, CH_3SiCl_3) was used for SiC coating deposition. Deposition experiments were performed in a hot-wall vertical reactor. Hydrogen was used as carrier gas, which delivered MTS through the bubbler to the reactor; argon was used as diluent and protective gas. The flow rate of hydrogen and argon was fixed at 200 sccm and 75 sccm (cm^3/min), respectively. The deposition was performed at 1000 °C for 2 h under a total pressure of 5.0 kPa.

Mu_f/Mu composites with SiC interphases (SiC–Mu_f/Mu composites) were fabricated via the sol–gel process. As shown in Fig. 1, the mullite sols were first infiltrated into mullite fiber preform in a vacuum apparatus at room temperature for 6 h, and then the preform was dried for 10 h at 80 °C to gel the mullite sols, and finally sintered at a heating rate of 10 °C/min up to 1200 °C for 1 h in argon atmosphere. This process was repeated 12 times to enhance the density of the composites.

2.3. Characterization of the materials

The density of the samples was measured according to Archimedes' Laws. Three-point bending tests were carried out at room temperature on samples with size of about $60^l \times 5^w \times 4^t$ mm^3. The gauge length was 50 mm and cross-head speed was 0.5 mm/min.

Morphology of the CVD SiC coatings and the composites after mechanical tests was observed by a scanning electron microscope (SEM, HITACHI FEG S4800). Phase compositions of mullite fibers, matrix and the composites were determined by X-ray diffraction (XRD) analysis using monochromatic Cu Kα radiation with a D8 ADVANCE diffractometer (Bruker, Germany). Surface of the pullout fibers in the composites was analyzed by EDS equipped with SEM. Infrared absorption spectra were recorded from 400 cm^{-1} to 1600 cm^{-1} with samples prepared by the KBr pellet method using an AVATAR 370 (Thermo Nicolet). Chemical components

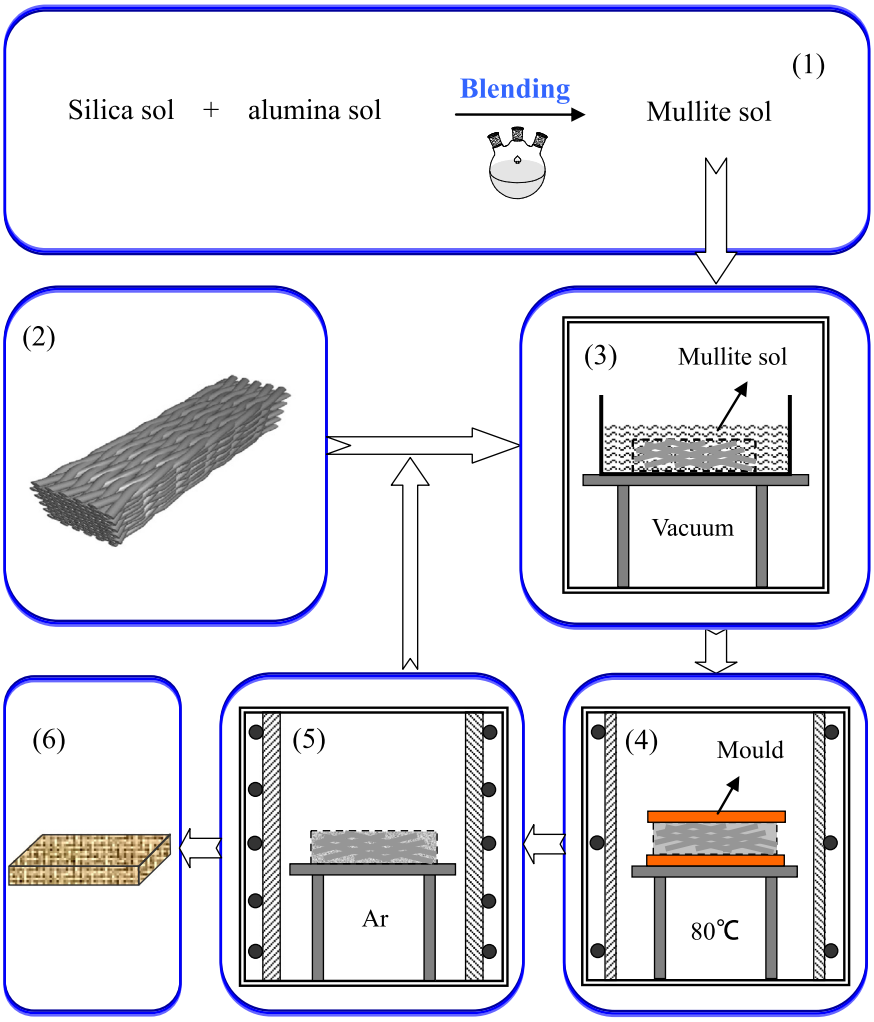

Fig. 1. Fabrication process of Mu_f/Mu composites with SiC interphases. (1) preparation of mullite sol; (2) preparation of mullite fiber preform with CVD SiC coatings; (3) infiltration of mullite sol; (4) gelation of mullite; (5) mullitization of matrix; (6) Muf/Mu composites with SiC interphases.

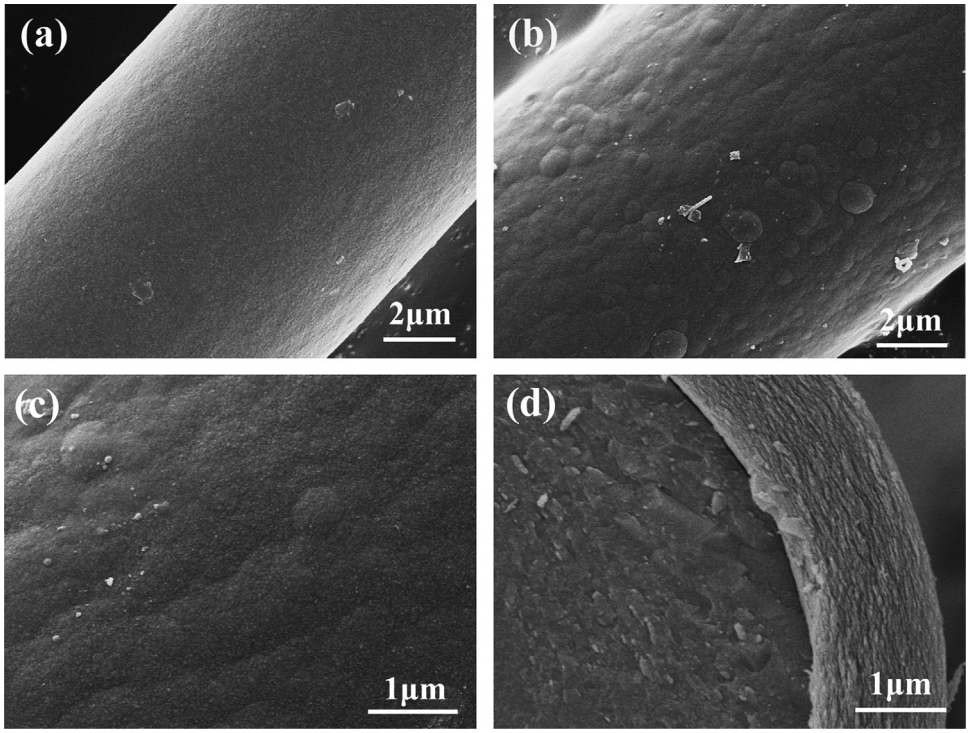

Fig. 2. SEM images of mullite fibers: (a) as-received and (b)–(d) with SiC coatings.

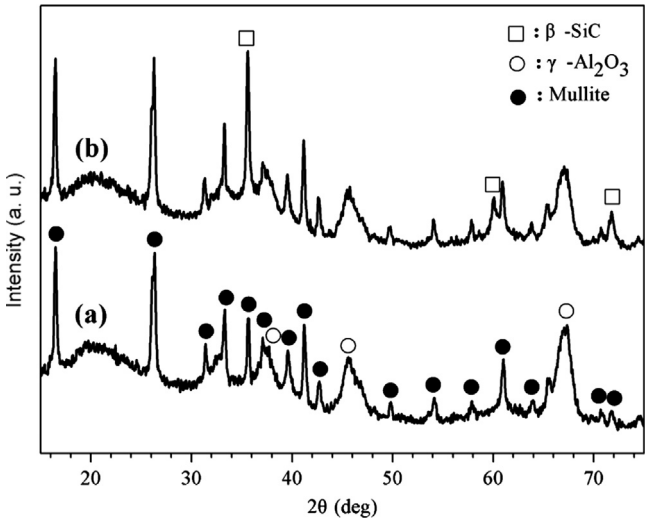

Fig. 3. XRD patterns of mullite fibers: (a) as-received and (b) with SiC coatings.

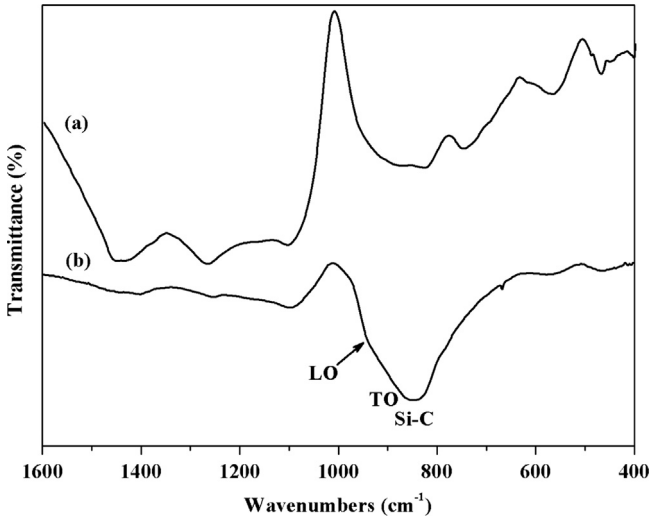

Fig. 4. FT-IR spectra of mullite fibers: (a) as-received and (b) with SiC coatings.

of the fibers were traced with X-ray photoelectron spectroscopy (XPS) analysis using a Thermo ESCALAB 250 apparatus with Al Kα radiation of energy 1486.6 eV.

3. Results and discussions

3.1. Characteristics of the CVD SiC coatings

Surface morphologies of mullite fibers with CVD SiC coatings are shown in Fig. 2b–d, and those of uncoated mullite fibers are shown in Fig. 2a for comparison. It can be seen that as-received fibers have smooth and homogeneous surface. After SiC coatings are deposited, some traces of strumae are observed on fiber surface (Fig. 2b and c). As shown in Fig. 2d, the SiC coating thickness is about 1.5 μm.

XRD pattern of mullite fibers with CVD SiC coatings is presented in Fig. 3b. For comparison, XRD pattern of as-received fibers is shown in Fig. 3a. Several XRD peaks are observed in Fig. 3a, which correspond to mullite and γ-Al_2O_3 phases. In Fig. 3b, three accessional obvious diffraction peaks at about the 2θ values of 35.60°, 60.06° and 71.83° (d=0.252, 0.154 and 0.131 nm) are detected, which correspond, respectively, to the (1 1 1), (2 2 0) and (3 1 1) reflections of β-SiC [13].

FT-IR spectra of mullite fibers are shown in Fig. 4. A narrow and sharpening absorption peak around 830 cm^{-1} and a shoulder near 940 cm^{-1} are detected for fibers with CVD SiC coatings, which are assigned to the transversal optic (TO) mode and the longitudinal optic (LO) mode of the SiC stretching vibration, respectively [14]. It is difficult to recognize the band near 1260 cm^{-1} due to Si–O–Si bond vibration in SiO_4 or Si–C bond stretch [15].

Examination of the XPS spectra around C 1s and Si 2p regions of the SiC coatings provides more details about the chemical components of the coatings. It can be seen from survey scan (Fig. 5a and b) that Al 2s and Al 2p peaks disappear for fibers with SiC coatings. The peaks positioned near 198 eV and 271 eV correspond to Cl $2p_{3/2}$ and Cl 2s, respectively, which indicate the absorption of HCl in CVD SiC coatings. Moreover, C 1s peak can be fitted into two sub-peaks at 282.6 eV and 283.2 eV (Fig. 5c), which should be assigned to C–Si and C–C bonds, respectively [16,17]. C–C bonds are attributed to free carbon in the coatings. The peak positioned at 100.9 eV in Si 2p spectra (as shown in Fig. 5d) is also identified as Si–C bond [18]. Hence, the above XRD, FT-IR and XPS results suggest that the carbon-rich β-SiC coatings are successfully prepared on mullite fibers by a CVD process.

3.2. Phase composition of Mu_f/Mu composites

XRD pattern of as-received Mu_f/Mu composites is shown in Fig. 6. It can be seen that the composites are composed of mullite, γ-Al_2O_3 and cristobalite phases. Hereinto, the major component is mullite, which contributes to good chemical and thermal resistance. Moreover, the phase developments of mullite fibers and gel-derived matrix during a heating process at fabrication temperature are also detected and shown in Fig. 7.

As shown in Fig. 7a, original fibers consist of γ-Al_2O_3 and amorphous silica. After heat-treatment at 1200 °C for 1 h, γ-Al_2O_3 reacts with amorphous silica to form orthorhombic mullite, the typical characterization of which is the splitting of (1 2 0) and (2 1 0) crystal planes at 2θ value of about 26° in XRD patterns [19]. As heat-treatment time is prolonged to 12 h, there is no change in phase structure but only enhancing of crystallinity degree and growing of mullite grains, which can be confirmed by the sharpening of (1 2 0) and (2 1 0) crystal planes (the insets of Fig. 7a) [20].

As shown in Fig. 7b, dried mullite gel is composed of bohemite. After heat-treatment at 1200 °C for 1 h, γ-Al_2O_3 is created. In addition, a wide peak is observed, suggesting that amorphous silica exists in the product. As heat-treatment time

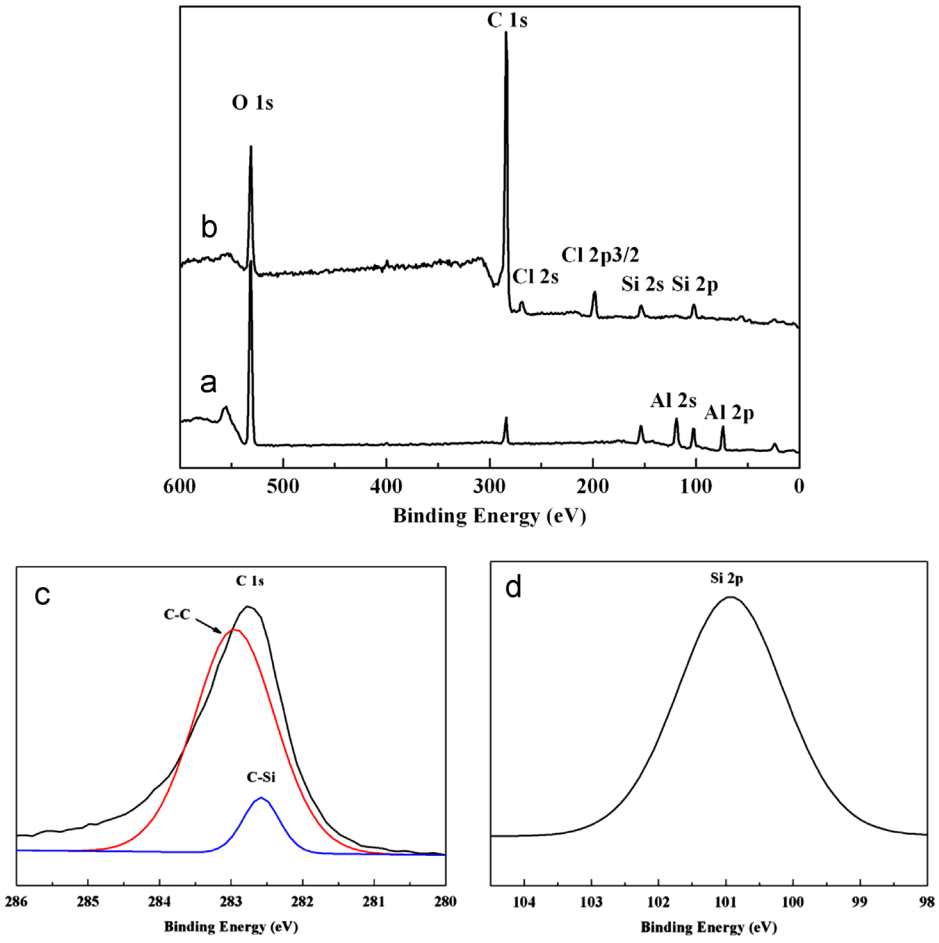

Fig. 5. XPS spectra of mullite fibers: (a) as-received and (b)–(d) with SiC coatings.

is prolonged to 12 h, γ-Al_2O_3 partially reacts with amorphous silica to form orthorhombic mullite, which is mainly controlled by the reaction dynamics mechanism. And the production mainly consists of mullite, γ-Al_2O_3 and amorphous silica. Besides, a trace of cristobalite originated from the crystallization of amorphous silica is also detected.

In general, under the condition that the inter-diffusion and reaction between mullite fiber and matrix are not evident and localized just at the fiber/matrix interface [21], it can be deduced that the mullite phase in the composites is ascribed to mullite fiber and gel-derived matrix, while γ-Al_2O_3 and cristobalite phases are mainly assigned to gel-derived matrix.

3.3. Mechanical properties of Mu_f/Mu composites

The flexural stress–displacement curves of Mu_f/Mu composites are shown in Fig. 8. Properties of the composites are summarized in Table 1. As shown in Fig. 8a, as-received composites exhibit an obvious brittle fracture behavior. In contrast, SiC–Mu_f/Mu composites show a standard toughened fracture behavior (Fig. 8b). When load reaches a maximum, it will not decrease sharply, but drop off gradually. The flexural strength of SiC–Mu_f/Mu composites is about 2.67 times that of as-received composites.

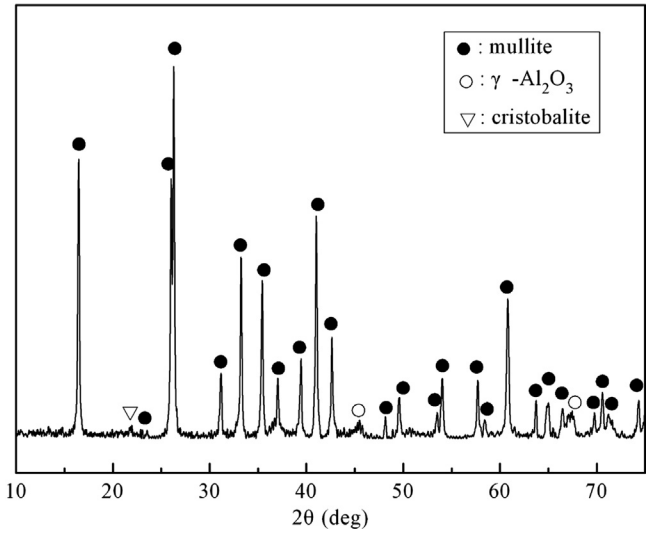

Fig. 6. XRD pattern of as-received Mu_f/Mu composites.

3.4. Microstructure of Mu_f/Mu composites

From the stress–displacement curves of the composites, it can be concluded that SiC interphases play a key part in improving mechanical properties of the composites. In order to investigate the effects of SiC interphases on mechanical properties of the composites, microstructure analysis is adopted by SEM.

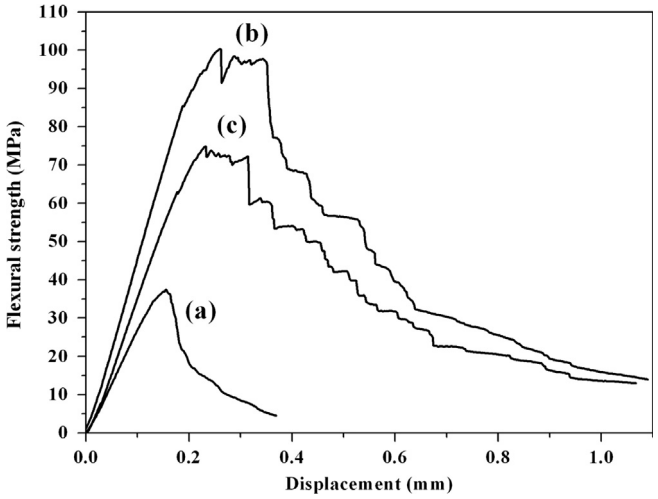

Fig. 8. Flexural stress–displacement curves of Mu_f/Mu composites: (a) as-received, (b) with SiC interphases, and (c) after thermal oxidation at 1200 °C for 4 h.

Table 1
Properties of Mu_f/Mu composites.

Samples	Original		After thermal oxidation		
	Density (g/cm^3)	Flexural strength (MPa)	Ratio of weight loss (%)	Density (g/cm^3)	Flexural strength (MPa)
As-received	2.07	37.51	0.85	2.10	36.67
SiC–Mu_f/Mu	1.97	100.33	2.68	1.85	74.83

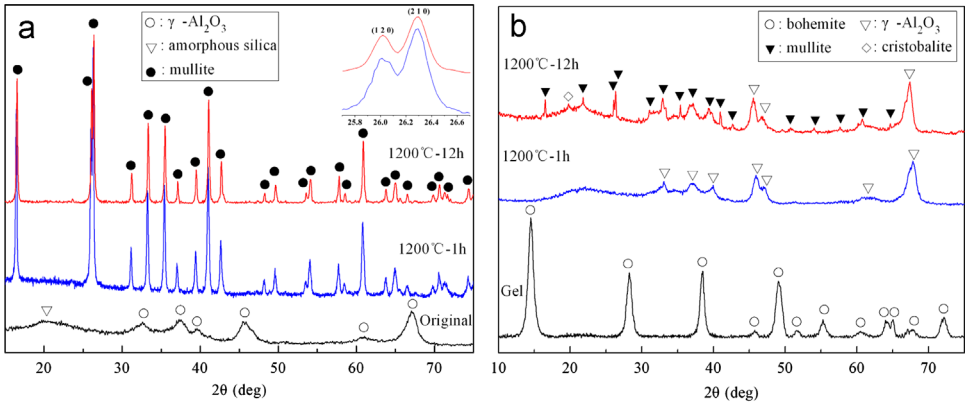

Fig. 7. Phase development of mullite fibers (a) and gel-derived matrix (b) during the heating process at 1200 °C.

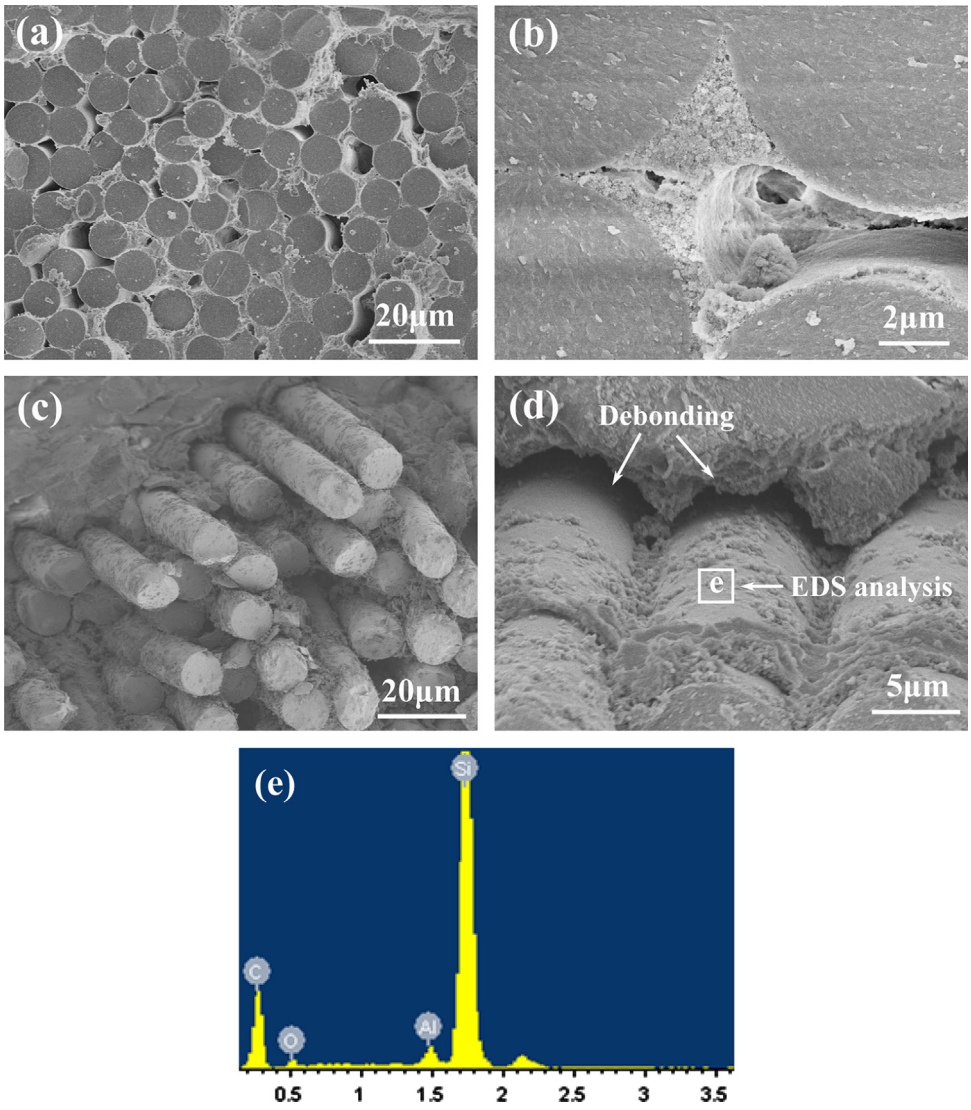

Fig. 9. Fracture surfaces of Mu_f/Mu composites: (a, b) as-received, (c, d) with CVD SiC interphases, and EDS analysis (e).

Fracture surfaces of Mu_f/Mu composites are shown in Fig. 9. For as-received composites, fracture surface is very even, and no pullout fibers can be found (Fig. 9a). As shown in Fig. 9b, mullite fibers were surrounded by mullite matrix tightly, and no interfacial debonding behaviors can be observed. Thus, the flexural strengths of the composites are low. Contrarily, for SiC–Mu_f/Mu composites, fracture surfaces show apparent fiber pullout (Fig. 9c), and the maximum length of the pullout fibers can exceed 40 μm. Surfaces of the pullout fibers are rough, and evident coatings surround the fibers. Interfacial debonding behaviors can be easily seen in Fig. 9d. When cracks extend into the SiC interphases, owing to their non-layered crystal structures, the cracks cannot deflect, but traverse the SiC interphases. Due to the relatively weak bonding between the SiC interphases and mullite fibers and matrix resulted from thermal mismatching, they will deflect at the interfaces either between the SiC interphases and mullite fibers or between SiC interphases and mullite matrix, which can both lead to interfacial debonding and fiber pullout in SiC–Mu_f/Mu composites.

Moreover, it can be seen from EDS analysis (Fig. 9e) that the bottom of the pullout fibers is surrounded with SiC coatings while no coatings exist on the top of the pullout fibers in SiC–Mu_f/Mu composites, which also proves that interfacial debonding occurs not only between SiC interphases and mullite fibers, but also between SiC interphases and mullite matrix.

3.5. Effects of thermal oxidation on mechanical properties of the composites

Although several researchers have confirmed that CVD SiC interphases show a good anti-oxidation capability [22,23] and Mu_f/Mu composites also have good oxidation resistance property [24], it is still necessary to evaluate the effects of thermal oxidation on mechanical properties of SiC–Mu_f/Mu composites as the SiC interphases prepared in this paper are rich in carbon.

The ratio of weight loss of the composites after thermal oxidation at 1200 °C for 4 h is shown in Table 1.

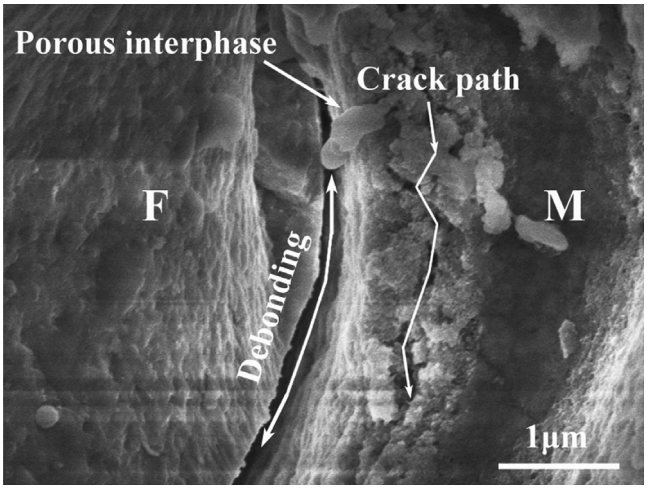

Fig. 10. Cross-sectional morphology of SiC–Mu_f/Mu composites after thermal oxidation at 1200 °C for 4 h.

It is observed that the ratio of weight loss of SiC–Mu_f/Mu composites is much higher (2.68%) than that of as-received composites (0.65%). The minor weight loss of the as-received composites comes mainly from two ways: 1) oxidation of the rudimental impurity from a desizing process and 2) volatilization of the absorbing water. From Fig. 8c, it can be seen that SiC–Mu_f/Mu composites after thermal oxidation still exhibit an obvious toughened fracture behavior. And the flexural strength of the composites is 74.6% of that of the original samples.

Fig. 10 shows cross-sectional morphology of SiC–Mu_f/Mu composites after thermal oxidation at 1200 °C for 1 h. It can be seen that the pores caused by carbon combustion are evident in SiC interphases. The bonding between matrix and interphase is tight, and matrix crack can effectively propagate to the SiC interphases and deflect between the pores in them. Moreover, interfacial debonding induced by a polishing process can be clearly seen between the fiber and interphases.

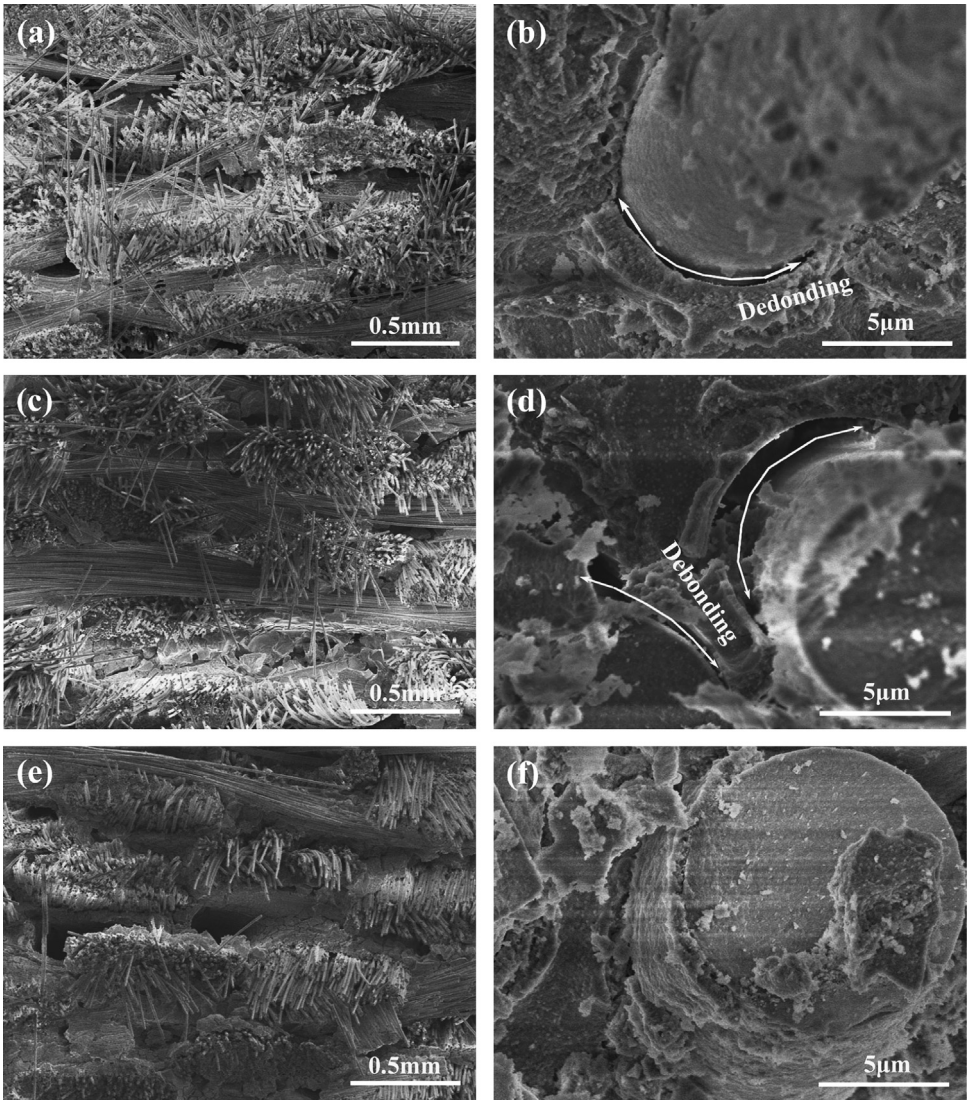

Fig. 11. Fracture surfaces of SiC–Mu_f/Mu composites after thermal oxidation at 1200 °C for 1 h (a, b), 4 h (c, d), and 8 h (e, f).

Fracture surfaces of SiC–Mu_f/Mu composites after thermal oxidation at 1200 °C for different times are shown in Fig. 11. It can be seen from lower magnification photographs (Fig. 11a, c and f) that the fiber pullout mechanism is evident for all the samples and the maximum length of the pullout fibers decreases with oxidation time increasing. Besides, different interfacial debonding behaviors can be seen from higher magnification photographs. As shown in Fig. 11b, the interfacial debonding occurs between the fiber and interphases, and the surface of the pullout fiber is smooth without any interphases. For the composites oxidized for 4 h (Fig. 11d), interfacial debonding occurs in SiC interphases, and the thickness of the coatings presented in matrix is uniform, while the coatings adhering to pullout fibers are porous and rough. Concerning the composites oxidized for 8 h (Fig. 11f), interfacial debonding is not evident, and the pullout fibers are surrounded tightly by the coatings. Therefore, it can be concluded that the interfacial bonding becomes stronger with oxidation time increasing, the reason for which may be the local SiC oxidation with SiO_2 glass formation on sides of the SiC coatings during heat-treatment at 1200 °C in air atmosphere [10].

As a matter of fact, the interfacial debonding/sliding resistance of SiC–Mu_f/Mu composites mainly depends on elastic modulus of the SiC coatings. Low elastic modulus significantly decreases the interfacial debonding/sliding resistance, and promotes fiber pullout. Elastic modulus is a function of porosity [25]:

$$E_p = E(1-1.9f_p+0.9f_p^2) \quad (1)$$

where E and E_p are the elastic modulus of the fully dense and porous materials, respectively, and f_p is the porosity. The elastic modulus of dense SiC is 185.0 GPa [26] assuming that the porosity of the SiC coatings after thermal oxidation is about 30%, and the elastic modulus is about 94.5 GPa. The decreasing of elastic modulus of the coatings favors the fiber pullout mechanism. Besides, during heat-treatment at 1200 °C, the local formation of SiO_2 glass by SiC oxidation will gradually decrease the coating porosity and thus increase the modulus of the SiC coatings. Then the fiber pullout mechanism will be limited. Therefore, due to the oxidation of SiC coatings and degradation of mullite fibers during the thermal oxidation process, the strength of SiC–Mu_f/Mu composites degraded after thermal oxidation.

4. Conclusions

Effects of the single layer CVD SiC interphases on mechanical properties and interfacial microstructure of Mu_f/Mu composites were investigated, and following conclusions can be reached:

(1) Uniform β-SiC fiber coatings about 1.5 μm thick are deposited on mullite fibers by the CVD process. Some traces of strumae are distributed on the fiber surface.
(2) Compared with as-received composites, Mu_f/Mu composites with CVD SiC interphases exhibit an obvious toughened fracture behavior, flexural strength of which is about 2.67 times that of as-received composites. The SiC interphases can provide protection for mullite fibers and appropriate interfacial bonding, which are both beneficial to the improvement in mechanical properties of Mu_f/Mu composites.
(3) The oxidation resistance of the composites with SiC interphases is a little weaker than those without SiC interphases. The strength of the composites after thermal oxidation at 1200 °C for 4 h degrades by about 25.4%.
(4) The interfacial bonding of the SiC–Mu_f/Mu composites becomes stronger with oxidation time increasing, the reason for which may be the local SiC oxidation with SiO_2 glass formation on sides of the SiC coatings during heat-treatment at 1200 °C in air atmosphere.

Acknowledgment

The authors appreciate the financial support of the National Natural Science Foundation of China (51202291), Aid Program for Innovative Group of National University of Defense Technology, and Aid program for Science and Technology Innovative Research Team in Higher Educational Institutions of Hunan Province.

References

[1] H. Schneider, S. Komarneni (Eds.), Mullite, WILEY-VCH Verlag GmbH & Co. KGaA, Weinheim, 2005.
[2] H. Schneider, J. Schreuer, B. Hildmann, Structure and properties of mullite—a review, Journal of the European Ceramic Society 28 (2008) 329–344.
[3] I.A. Aksay, D.M. Dabbs, M. Sarikaya, Mullite for structural, electronic, and optical applications, Journal of the American Ceramic Society 74 (1991) 2343–2358.
[4] Q.S. Ma, Z.H. Chen, W.W. Zheng, H.F. Hu, Fabrication and mechanical properties of three-dimensional carbon fibre reinforced mullite composites via sol–gel, Rare Metal Materials and Engineering 33 (2004) 111–114.
[5] Y. Yoshiaki, K. Yoshiaki, T. Nobuo, K. Teruo, Interfacial debonding behavior of mullite/SiC continuous fiber composite, Journal of the American Ceramic Society 78 (1995) 3209–3216.
[6] B. Kanka, H. Schneider, Aluminosilicate fiber/mullite matrix composites with favorable high-temperature properties, Journal of the European Ceramic Society 20 (2000) 619–623.
[7] C. Kaya, E.G. Butler, A. Selcuk, et al., Mullite (Nextel™ 720) fibre-reinforced mullite matrix composites exhibiting favourable thermomechanical properties, Journal of the European Ceramic Society 22 (2002) 2333–2342.
[8] E. Mouchon, P. Colomban, Oxide ceramic matrix/oxide fibre woven fabric composites exhibiting dissipative fracture behavior, Composites 26 (1995) 175–182.
[9] M. Schmücker, F. Flucht, P. Mechnich, Degradation of oxide fibers by thermal overload and environmental effects, Materials Science and Engineering A 557 (2012) 10–16.
[10] M. Schmücker, H. Schneider, K.K. Chawla, et al., Thermal degradation of fiber coatings in mullite-fiber-reinforced mullite composites, Journal of the American Ceramic Society 80 (1997) 2136–2140.
[11] J.H. Weaver, J. Yang, F.W. Zok, Control of interface properties in oxide composites via fugitive coatings, Journal of the American Ceramic Society 91 (2008) 4003–4008.
[12] J.B. Davis, D.B. Marshall, P.E.D. Morgan, Monazite-containing oxide/oxide composites, Journal of the European Ceramic Society 20 (2000) 583–587.

[13] H.T. Liu, H.F. Cheng, J. Wang, et al., Effects of the single layer CVD SiC interphases on the mechanical properties of the SiCf/SiC composites fabricated by PIP process, Ceramics International 36 (2010) 2033–2037.
[14] Y.H. Baek, Y.H. Ryu, K.J. Yong, Structural characterization of β-SiC nanowires synthesized by direct heating method, Materials Science and Engineering C 26 (2006) 805–808.
[15] P. Padmaja, G.M. Anilkumar, P. Mukundan, et al., Characterisation of stoichiometric sol–gel mullite by Fourier transform infrared spectroscopy, International Journal of Inorganic Materials 3 (2001) 693–698.
[16] H.T. Liu, H.F. Cheng, J. Wang, et al., Dielectric properties of the SiC fiber-reinforced SiC matrix composites with the CVD SiC interphases, Journal of Alloys and Compounds 491 (2010) 248–251.
[17] D. Dietrich, P.W. Martin, K. Nestler, et al., Transmission electron microscopic investigations on SiC- and BN-coated carbon fibres, Journal of Materials Science 31 (1996) 5979–5984.
[18] H.T. Liu, H.F. Cheng, J. Wang, et al., Effects of the fiber surface characteristics on the interfacial microstructure and mechanical properties of the KD SiC fiber reinforced SiC matrix composites, Materials Science and Engineering A 525 (2009) 121–127.
[19] E.R. de Sola, F.J. Serrano, F.J. Torres, et al., An X-ray powder diffraction study of the microstructural evolution on heating 3:2 and 2:1 mullite single-phase gels, Crystal Research Technology 41 (2006) 1036–1044.
[20] Y. Wang, H.F. Cheng, H.T. Liu, et al., Microstructure and room temperature mechanical properties of mullite fibers after heat-treatment at elevated temperatures, Materials Science and Engineering A 578 (2013) 287–293.
[21] M. Schmücker, P. Mechnich, Improving the microstructural stability of Nextel™ 610 alumina fibers embedded in a porous alumina matrix, Journal of the American Ceramic Society 93 (2010) 1888–1890.
[22] Y. Xiang, W. Li, S. Wang, et al., Effects of the single layer CVD SiC interphases on the mechanical properties of the C/SiC composites fabricated by PIP process, Materials Science and Engineering A 558 (2012) 451–455.
[23] S.A. Chen, Y.D. Zhang, C.R. Zhang, et al., Effects of SiC interphase by chemical vapor deposition on the properties of C/ZrC composite prepared via precursor infiltration and pyrolysis route, Materials and Design 46 (2013) 497–502.
[24] M.L. Antti, E.L. Curzio, R. Warren, Thermal degradation of an oxide fibre (Nextel 720)/aluminosilicates composite, Journal of the European Ceramic Society 24 (2004) 565–578.
[25] Y.H. Bao, P.S. Nicholson, $AlPO_4$-coated mullite/alumina fiber reinforced reaction-bonded mullite composites, Journal of the European Ceramic Society 28 (2008) 3041–3048.
[26] S. Kumar, R.N. Singh, Effects of coating properties on crack propagation in Nicalon-fiber/SiC-matrix composites, Composites Science and Technology 56 (1996) 1271–1281.